



日本原子力研究開発機構機関リポジトリ
Japan Atomic Energy Agency Institutional Repository

Title	^{29}Si NMR spin-echo decay in YbRh_2Si_2
Author(s)	Kambe Shinsaku, Sakai Hironori, Tokunaga Yo, Hattori Taisuke, Lapertot G., Matsuda Tatsuma, Knebel G., Flouquet J., Walstedt R. E.
Citation	Journal of Physics; Conference Series,683(1),p.012006_1-012006_7
Text Version	Published Journal Article
URL	https://jopss.jaea.go.jp/search/servlet/search?5053243
DOI	https://doi.org/10.1088/1742-6596/683/1/012006
Right	Content from this work may be used under the terms of the Creative Commons Attribution 3.0 licence . Any further distribution of this work must maintain attribution to the author(s) and the title of the work, journal citation and DOI. Published under licence by IOP Publishing Ltd

^{29}Si NMR spin-echo decay in YbRh_2Si_2

This content has been downloaded from IOPscience. Please scroll down to see the full text.

2016 J. Phys.: Conf. Ser. 683 012006

(<http://iopscience.iop.org/1742-6596/683/1/012006>)

View [the table of contents for this issue](#), or go to the [journal homepage](#) for more

Download details:

IP Address: 133.53.248.253

This content was downloaded on 08/02/2016 at 01:09

Please note that [terms and conditions apply](#).

^{29}Si NMR spin-echo decay in YbRh_2Si_2

S. Kambe¹, H. Sakai¹, Y. Tokunaga¹, T. Hattori¹, G. Lapertot², T.D. Matsuda³, G. Knebel², J. Flouquet², and R.E. Walstedt⁴

¹Advanced Science Research Center, Japan Atomic Energy Agency, Tokai-mura, Ibaraki 319-1195, Japan

²SPSMS/CEA-Grenoble, 38000 Grenoble, France

³Division of Physics, Tokyo Metropolitan University, Hachioji-shi, Tokyo 192-0397, Japan

⁴Physics Department, The University of Michigan, Ann Arbor, MI 48109, USA

E-mail: kambe.shinsaku@jaea.go.jp

Abstract. ^{29}Si nuclear magnetic resonance (NMR) has been measured in a ^{29}Si -enriched single crystal sample of YbRh_2Si_2 . The spin-echo decay for applied field $H \parallel, \perp$ the c -axes has been measured at 100 K. A clear spin-echo decay oscillation is observed for both cases, possibly reflecting the Ruderman-Kittel (RK) interaction. Since the observed oscillation frequency depends on the direction of applied magnetic field, anisotropic RK coupling and pseudo-dipolar (PD) interactions may not be negligible in this compound. The origin of spin-echo decay oscillations is discussed.

1. Introduction

The quantum critical phase transition (QCPT) is one of the important aspects of Kondo lattices at low temperatures. In YbRh_2Si_2 [1], the QCPT is not a case of the ordinary spin density wave (SDW) instability observed in Ce-based Kondo-lattices [2], but a candidate for a novel case of local criticality [3]. In YbRh_2Si_2 , the weak antiferromagnetic transition below $T_N \sim 70$ mK is easily tuned to $T = 0$ with a small applied magnetic field H [1]. At the critical magnetic field H_{cr} for $T_N \sim 0$ K, the T -dependence of the physical properties shows non-Fermi liquid (NFL) behavior owing to quantum critical fluctuations that occur on approaching the QCPT [4]. Having a tetragonal crystal structure (Fig. 1), YbRh_2Si_2 exhibits an anisotropic electronic state [5]. Thus, for applied field $H \perp$ and \parallel the c -axis, the critical field is $H_{cr} \sim 0.06$ T and ~ 0.66 T, respectively, indicating that the effective energy scale for quantum criticality is ~ 10 times larger for $H \parallel$ the c -axis. In a previous study of the spin-lattice relaxation time T_1 as a function of temperature and field, we reported that coexisting, degenerate Fermi and non-Fermi liquid states appeared around the QCPT [6]. In a fashion similar to H_{cr} , the coexisting states showed rather anisotropic behavior [7, 8].

In the present study, we report data for the ^{29}Si nuclear spin-echo decay in YbRh_2Si_2 . Here, we have chosen to apply H parallel and perpendicular to the c -axes in order to investigate the anisotropy of the electronic state. The observed spin-echo decay curves show a clear oscillation, which may be due to the Ruderman-Kittel (RK) interaction [9]. The anisotropic oscillation frequency indicates that the contribution of the pseudo-dipolar (PD) interaction [10] is not negligible, an effect that may also reflect the anisotropy of the electronic state.

The low natural abundance ($\sim 4.7\%$) of ^{29}Si ($I = 1/2$; $\gamma_n/(2\pi) = 845.77$ Hz/Oe; γ_n : gyromagnetic ratio; $\omega_n = \gamma_n H$ corresponds to the NMR measurement frequency) has prevented



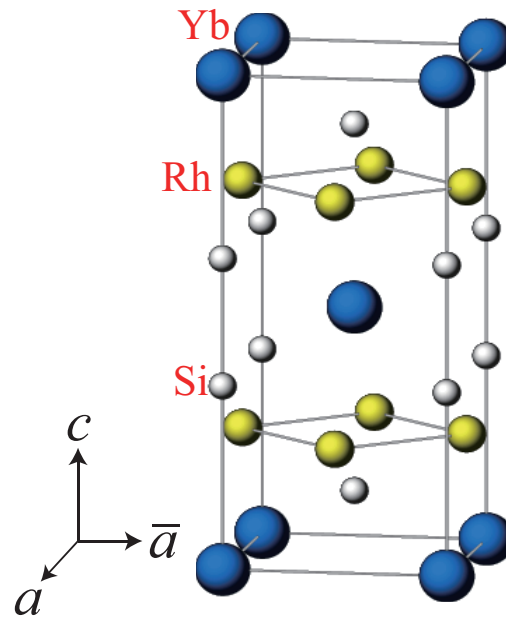


Figure 1. Tetragonal crystal structure ($I4/mmm$) of YbRh_2Si_2 . The local symmetry of the Si site is tetragonal $4mm$.

highly accurate ^{29}Si NMR measurements on YbRh_2Si_2 up to now. For the present study a single crystal sample has been prepared with the ^{29}Si isotope enriched to 52 %, improving the NMR sensitivity by a factor ~ 11 .

2. Experimental

Single crystals of YbRh_2Si_2 were grown by the In-flux method. The starting materials were Yb, Rh, natural Si, 99.3 % enriched ^{29}Si and In. These materials were put in an alumina crucible and sealed in a quartz tube with the stoichiometric composition of $\text{Yb}:\text{Rh}:\text{Si}:\text{Si}^{29}:\text{In} = 1:2:1:1:65$. The ampoule was heated up to 1200 °C, maintained at this temperature for one day, and cooled to 900 °C at a rate of 1 °C/h, taking about 14 days in total. The excess flux was removed from the crystals by spinning the ampoule in a centrifuge.

High sample purity was confirmed by the small residual resistivity $\rho_0 \sim 0.99 \mu\Omega\text{cm}$ and the large RRR value $=\rho(300\text{K})/\rho(2\text{K}) = 104$. No magnetic impurity phase was detected in magnetic susceptibility measurements. The antiferromagnetic phase transition was observed near 80 mK at zero field.

A single crystal specimen ($6 \times 3 \times 0.1 \text{ mm}^3$) was mounted in a ^4He cryostat with an NMR pickup coil. Using a standard $\pi/2 - \pi$ pulse sequence, the spin-echo intensity $m(2\tau)$ so generated was measured as a function of the time τ between the pulses for the measurement of the spin-echo decay (see Fig. 2 a). Here, a typical $\pi/2$ pulse width is $4 \sim 5 \mu\text{sec}$. Since the resonance linewidth is quite narrow (*e.g.* $\sim 9 \text{ kHz}$ at 7.2 T), all nuclear spins in the spectrum were quite uniformly excited by the radio-frequency pulses used. The pulse repetition time t_{rep} was taken to be much longer than the previously determined T_1 [6, 7, 8]. Figure 2b) shows a calculated typical spin-echo decay curve without the oscillation term. (See below: This case is from Eqs. 2 and 4 with $J = 0$, *i.e.* $W(2\tau)/W(0) = 1$). Here we have adopted the values $1/T_{1L} = 15 \text{ sec}^{-1}$ and $1/T_{2G} = 470 \text{ sec}^{-1}$, which are similar values to those in the $H \parallel c$ case shown below.

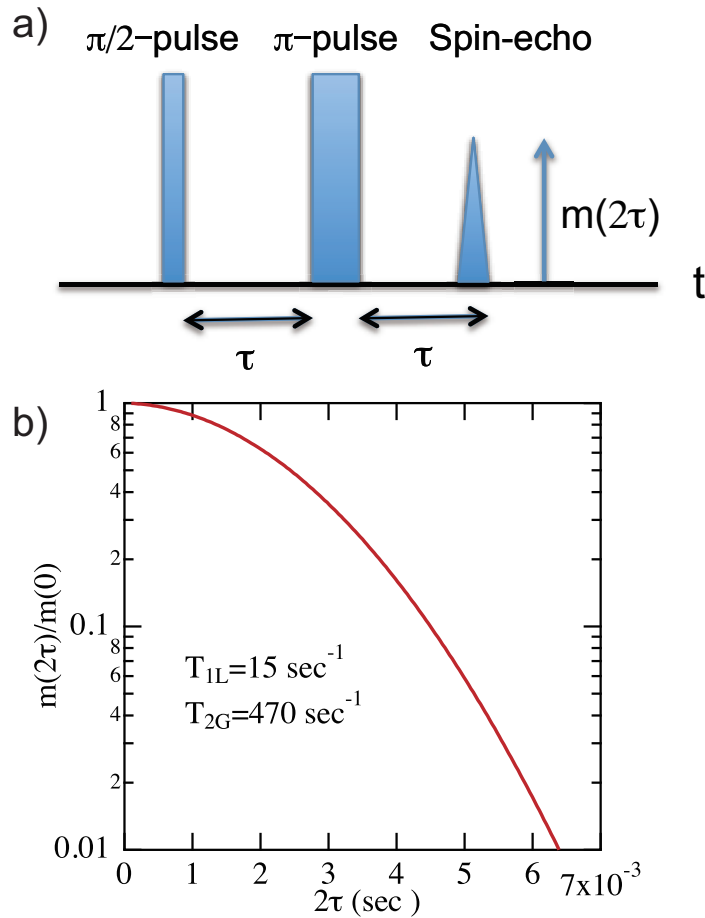


Figure 2. a) Schematic description of NMR spin-echo formation. In the present case, typical τ is considerably larger than the π -pulse width ($\sim 10^{-5}$ sec). b) Calculated spin-echo decay curve without oscillation term ($J = 0$ case for Eqs. 2 and 4). We adopt similar $1/T_{1L} = 15 \text{ sec}^{-1}$ and $1/T_{2G} = 470 \text{ sec}^{-1}$ values to these in the $H \parallel c$ case (see Table 1). In the real case for $H \parallel c$ with $J > 0$, the calculated curve is modulated with the $W(2\tau)/W(0)$ term as shown in Fig. 3 b).

In the actual case with $J > 0$, the spin-echo decay curve is modified by the oscillation factor $W(2\tau)/W(0)$.

3. Spin-echo oscillation due to RK interactions

It is well known that the RK interaction can induce oscillations in the spin-echo decay curve [9]. In the present analysis, the question of PD interaction effects is set aside, though it will be mentioned below. In metals the indirect RK interaction between nuclear spins $\mathbf{I}_i, \mathbf{I}_j$ occurs through second-order scattering of conduction electrons [11], taking the scalar form

$$J_{ij} \mathbf{I}_i \cdot \mathbf{I}_j. \quad (1)$$

The magnitude of J_{ij} can be estimated from the oscillation frequency of the spin-echo envelope [9]. In fact, this type of oscillation has been observed in Pt alloys [9]. Spin-echo oscillations due to RK interactions are predominant if the following conditions are satisfied: a) dipolar and PD

Table 1. Values of $1/T_{2G}$ and J obtained from fits, along with previously determined $1/T_1$ values [6, 7, 8], which are adopted as $1/T_{1L}$.

	$1/T_{1L}$ (sec ⁻¹)	$1/T_{2G}$ (sec ⁻¹)	$J/2\pi$ (kHz)
$H \parallel c$	15	470 ± 10	1.07 ± 0.02
$H \perp c$	12.9	522 ± 10	0.50 ± 0.01

interactions can be neglected; and b) local inhomogeneous broadening is larger than the indirect RK interaction [9]. Condition a) is considered to be satisfied in the present case. The lattice sum of nuclear dipolar field at the Si site in YbRh₂Si₂ is estimated as ~ 0.1 Oe, which corresponds to $\sim 0.1 \times \gamma_n/(2\pi) \cong 85$ Hz. This is much smaller than the estimated RK interaction (see below). The PD interaction is not negligible, a point to be discussed later. Condition b) is satisfied, since the observed inhomogeneous linewidth ~ 9 kHz at 7.2 T is much larger than the estimated RK interaction.

An RK oscillation factor $W(2\tau)$ for the spin echo ($I = 1/2$ nuclei, $\pi/2 - \pi$ pulses) is analyzed here considering only the nearest-neighbor (nn) nuclear spins, *i.e.* $J_{ij} = J$. Then, we adopt the expression [12]

$$W(2\tau) = \sum_{r=0}^N A_r \cos^r(J\tau), \quad (2)$$

where A_r is the probability that a ²⁹Si nucleus has r nn ²⁹Si, and $N = 4$ is the total number of nn Si sites in YbRh₂Si₂.

If conditions a) and b) are satisfied, with ²⁹Si nuclei distributed randomly, A_r may be expressed by the binomial coefficient $\binom{N}{r}$ with concentration p of ²⁹Si nuclear species,

$$A_r = A_{rnn} \equiv \binom{N}{r} p^r (1-p)^{N-r}. \quad (3)$$

If in addition to the oscillation factor $W(2\tau)$ there is a spin-lattice relaxation time $T_{1L} \approx T_1$ and a Gaussian component of spin-spin relaxation time T_{2G} , then the observed 2τ dependence of spin-echo intensity $m(2\tau)$ may be expressed,

$$\frac{m(2\tau)}{m(0)} = \exp\left\{-\frac{2\tau}{T_{1L}} - \frac{1}{2} \left(\frac{2\tau}{T_{2G}}\right)^2\right\} \frac{W(2\tau)}{W(0)}. \quad (4)$$

In the present study data for spin-echo decay curves has been analyzed based on this equation.

4. Results and discussion

Figure 3 shows spin-echo decay data for $H = 7.2 T \parallel, \perp$ c-axis at 100 K. Since the local site symmetry for Si is tetragonal $4mm$, no anisotropy is observed for applied field in the (001) plane. At this temperature Yb magnetic moments are considered to have strongly localized character [6, 7, 8], since the spin-lattice relaxation time T_1 is almost independent of T . Figure 4 shows spin-echo decay with different second-pulse widths for $H = 7.2 T \parallel$ c-axis at 100 K. As the second pulse width decreases, the spin-echo decay becomes slower, indicating that the spin-echo

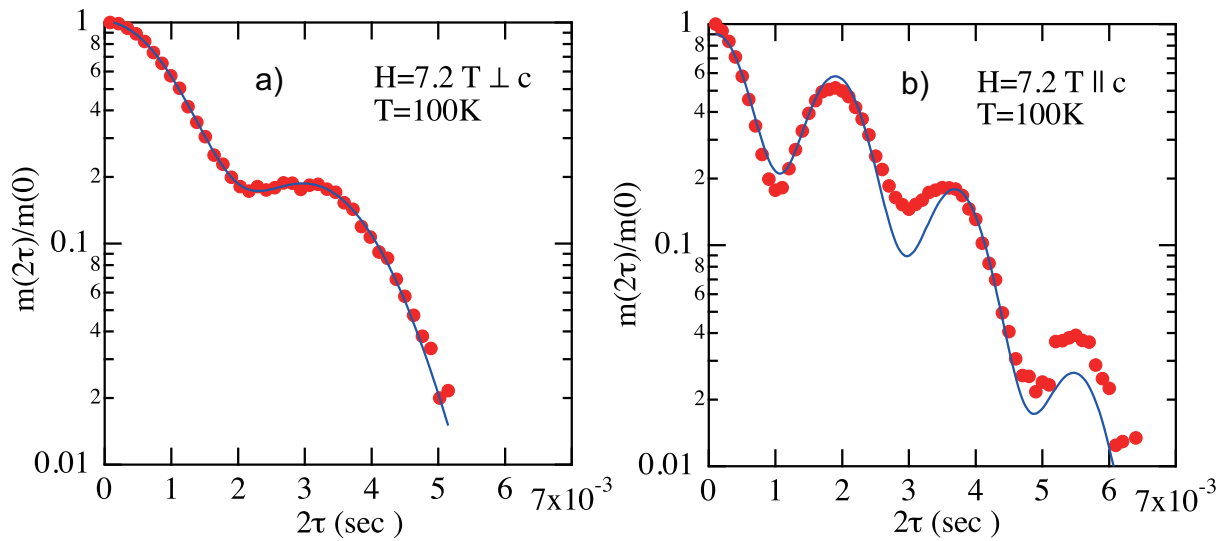


Figure 3. Spin-echo decay curves for a $\pi/2 - \pi$ pulse sequence at $H = 7.2\text{T} \parallel, \perp$ the c -axis at 100 K. Solid lines were obtained using least square fits based on Eqs. 2 and 4.

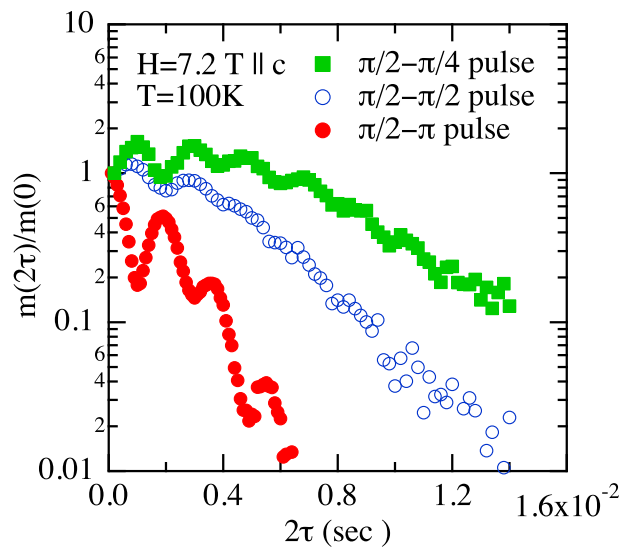


Figure 4. Spin-echo decay curves with different pulse sequences for $H = 7.2\text{T} \parallel, \perp$ c -axis at 100 K. As the second pulse width decreases, the spin-echo decay becomes substantially slower, indicating that the spin-echo decay is static, *i.e.* driven by the π pulse, aside from the T_{1L} process.

decay process is dominated by pulse modulation of static couplings, except for the (weak) T_{1L} relaxation process. In this situation, the echo is relaxed by the reorientation of neighbor spins by the refocusing second pulse. As is clearly seen in Fig. 3, the oscillation frequency is larger for $H \parallel c$ than $H \perp c$. The echo-decay curves are fitted using Eq. 4. Here the previously determined $1/T_1$ values [6, 7, 8] have been adopted as $1/T_{1L}$. Parameters J , A_r and $1/T_{2G}$ have been optimized with least-squares fits. Values of $1/T_{2G}$ and J so obtained are presented in

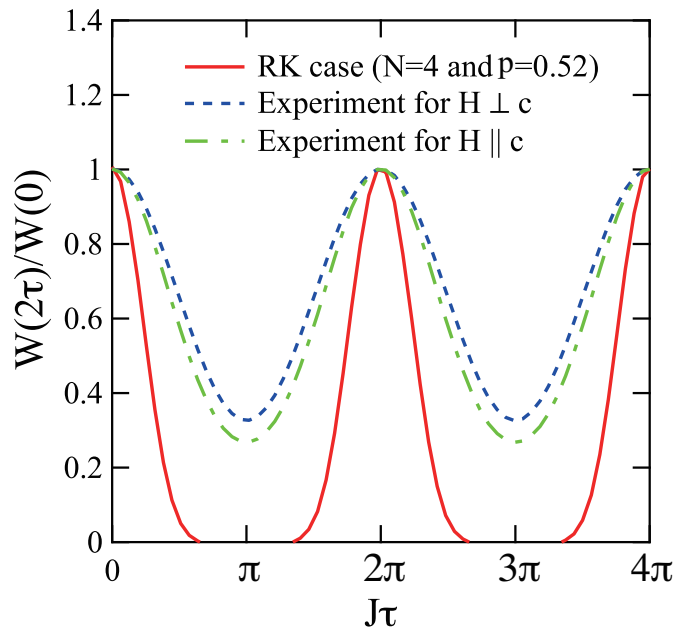


Figure 5. Normalized oscillation factor for spin-echo decay $W(2\tau)/W(0)$. Solid line corresponds to the ideal RK case expressed by Eq. 2 with $N = 4$ and $p = 0.52$. Dashed and broken lines are obtained by fitting to the results presented in Fig. 3 using Eqs. 2 and 4. Deviations from the solid line indicate either that the RK interaction is anisotropic in tetragonal symmetry or that the PD interaction is not negligible.

Table. 1. Since the value deduced for A_r is somewhat different from $A_{r_{bn}}$, the value obtained for $W(2\tau)$ is slightly different from the ideal RK case as shown in Fig. 5. These deviations indicate that either RK coupling is anisotropic or PD contributions are appreciable. Such effects have been observed in previous studies [12].

In contrast to the scalar RK interaction (Eq. 1), the PD interaction is a tensor quantity [12],

$$B_{ij}(\mathbf{I}_i \cdot \mathbf{I}_j - 3I_j^z I_k^z), \quad (5)$$

$$B_{ij} = \frac{1}{2} b_{ij} (3\cos^2\theta_{ij} - 1), \quad (6)$$

where r_{ij} is the distance between the i th and the j th nuclei, θ_{ij} is the angle between r_{ij} and the applied magnetic field, and b_{ij} is the effective coefficient for dipolar-type interaction B_{ij} between the i th and j th nuclei. Thus, the PD interaction depends on the direction of applied field. If the PD interaction is included, the observed τ -dependence of $W(2\tau)$ can be accounted for better. However, the observed oscillation frequency may not correspond to J exactly, and the real J value may be somewhat larger than the one given here [12].

In the present study, the anisotropic response of J against applied field is suggested. However, in the present RK and PD models (Eqs. 1 and 6), the crystal *i.e.* tetragonal anisotropy is not included explicitly. It is necessary to consider a relevant model for tetragonal system such as YbRh_2Si_2 in order to estimate J and B_{ij} more precisely. Principally, the anisotropy of J reflects the anisotropy of the Fermi-surface shape. Further analysis based on an improved model will be presented elsewhere.

Acknowledgments

We are grateful for stimulating discussions with S. Watanabe, K. Izawa, K. Ishida, H. Ikeda, J.-P. Brison, Y.-F. Yang, Z. Fisk and K. Kubo. A part of this work was supported by a Grant-in-Aid for Scientific Research on Innovative Areas Heavy Electrons (No. 20102006 and No. 20102007) from the MEXT, and the REIMEI Research Program of JAEA.

- [1] Gegenwart P, Custers J, Geibel C, Neumaier K, Tayama T, Tenya K, Trovarelli O and Steglich F 2002 *Phys. Rev. Lett.* **89** 056402.
- [2] Millis A J 1993 *Phys. Rev. B* **48** 7183.
- [3] Si Q, Rabello S, Ingersent K and Smith J L 2001 *Nature* (London) **413** 804.
- [4] Trovarelli O, Geibel C, Mederle S, Langhammer C, Groshe F M, Gegenwart P, Lang M, Sparn G and Steglich F 2000 *Phys. Rev. Lett.* **85** 626.
- [5] Custers J, Gegenwart P, Wilhelm H, Neumaier K, Tokiwa Y, Trovarelli O, Geibel C, Steglich F, Pépin C and Coleman P 2003 *Nature* (London) **424** 524.
- [6] Kambe S, Sakai H, Tokunaga Y, Lapertot G, Matsuda T D, Knebel G, Flouquet J and Walstedt R.E. 2014 *Nature Physics* **10** 840.
- [7] Kambe S, Sakai H, Tokunaga Y, Lapertot G, Matsuda T D, Knebel G, Flouquet J and Walstedt R.E. 2015 *Phys. Rev. B* **91** 161110(R).
- [8] Kambe S, Sakai H, Tokunaga Y, Lapertot G, Matsuda T D, Knebel G, Flouquet J and Walstedt R.E. 2015 *J. Phys. Conf. Series* **592** 012085.
- [9] Froidevaux C. and Weger M. 1964 *Phys. Rev. Lett.* **12** 123.
- [10] Bloembergen N. and Rowland T. J. 1955 *Phys. Rev.* **97** 1679.
- [11] Ruderman M. A. and Kittel C. 1954 *Phys. Rev.* **96** 99.
- [12] Alloul H. and Froidevaux C. 1967 *Phys. Rev.* **163** 324.